JOC Article
pubs.acs.org/joc

Competing Pathways in the Photo-Favorskii Rearrangement and Release of Esters: Studies on Fluorinated *p*-Hydroxyphenacyl-Caged GABA and Glutamate Phototriggers

Kenneth Stensrud,[†] Jihyun Noh,[‡] Karl Kandler,[‡] Jakob Wirz,[§] Dominik Heger,[⊥] and Richard S. Givens*,[†]

[†]*Department of Chemistry, 1251 Wescoe Hall Drive, University of Kansas, Lawrence, Kansas 66045,* [‡]*Department of Otolaryngology, 3500 Terrace Street, University of Pittsburgh, Pittsburgh, Pennsylvania 15208,* [§]*Departement Chemie, Universität Basel, Klingelbergstrasse 80, CH-4056 Basel, Switzerland, and* [⊥]*Department of Chemistry, Faculty of Science, Masaryk University, Brno, Czech Republic*

givensr@ku.edu

Received January 26, 2009

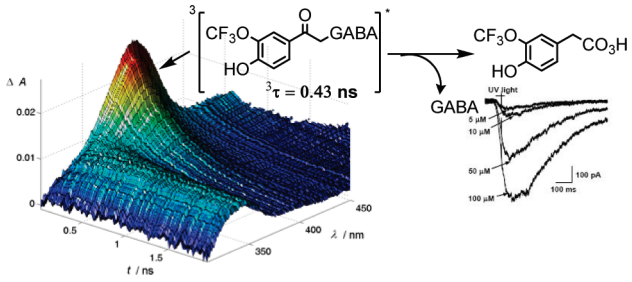

Three new trifluoromethylated *p*-hydroxyphenacyl (pHP)-caged γ-aminobutyric acid (GABA) and glutamate (Glu) derivatives have been examined for their efficacy as photoremovable protecting groups in aqueous solution. Through the replacement of hydrogen with fluorine, e.g., a *m*-trifluoromethyl or a *m*-trifluoromethoxy versus *m*-methoxy substituents on the pHP chromophore, modest increases in the quantum yields for the release of amino acids GABA and glutamate as well as improved lipophilicity were realized. The pHP triplet undergoes a photo-Favorskii rearrangement with concomitant release of the amino acid substrate. Deprotonation competes with the rearrangement from the triplet excited state and yields the pHP conjugate base that, upon reprotonation, regenerates the starting ketoester, a chemically unproductive or "energy-wasting" process. When picosecond pump−probe spectroscopy is employed, GABA derivatives **2**−**5** are characterized by short triplet lifetimes, a manifestation of their rapid release of GABA. The bioavailability of released GABA at the $GABA_A$ receptor improved when the release took place from *m*-OCF_3 (**2**) but decreased for *m*-CF_3 (**3**) when compared with the parent pHP derivative. These studies demonstrate that pK_a and lipophilicity exert significant but sometimes opposing influences on the photochemistry and biological activity of pHP phototriggers.

Introduction

Photoremovable protecting groups or "phototriggers" have found many applications in chemistry and biology and have become a subject of wide interest.[1,2] They diminish or block the normal reactivity of an active compound, which can be restored upon exposure to light. When employed in this capacity, light is regarded as a "traceless reagent" that can be administered along specific spatial, temporal, and concentration coordinates.[1,3] These features are exploited, for example, through the release of the carboxyl group of the amino acids glutamate (Glu), γ-aminobutyric acid (GABA),

(1) (a) *Dynamic Studies in Biology, Phototriggers, Photoswitches, and Caged Compounds*; Goeldner, M., Givens, R., Eds.; Wiley-VCH: Weinheim, Germany, 2005. (b) Pelliccioli, A. P.; Wirz, J. *Photochem. Photobiol. Sci.* **2002**, *1*, 441–458. (c) Adams, S. R.; Tsien, R. Y. *Annu. Rev. Physiol.* **2000**, *18*, 755–784.

(2) (a) *Greene's Protective Groups in Organic Synthesis*, 4th ed.; Wutts, P. G. M., Greene, T. W., Eds.; Wiley Interscience−John Wiley and Sons: New York, 2007; pp 980−9832. (b) Protti, S.; Fagnoni, M. *Chem. Commun.* **2008**, 3611–3621.

(3) Ni, J.; Auston, D. A.; Frelich, D. A.; Muralidharan, S.; Sobie, E. A.; Kao, J. P. Y. *J. Am. Chem. Soc.* **2007**, *129*, 5316–5317.

DOI: 10.1021/jo900139h Published on Web 07/02/2009

or glycine in order to investigate neuronal processes in cell-signaling, kinetic, and mechanistic studies of the central nervous system.[4]

Since our discovery that the *p*-hydroxyphenacyl (pHP) chromophore will serve as a photoremovable protecting group,[5] several biologically relevant substrates such as phosphates (ATP[5] and GTP[6]), thiols (Protein Kinase A[7] and glutathione[8]), and carboxylates (GABA[9] and Glu[10]), including the C terminus of the oligopeptide (bradykinin[11,12]) and examples of functional group protection in synthesis[2], have been reported. This has prompted us to investigate the mechanistic features and substituent effects on the reaction. Interestingly, the reaction results in a significant and useful[13] blue shift because of the rearrangement of the chromophore to (*p*-hydroxyphenyl)acetic acid (**6**) as a primary product (eq 1). The reaction mechanism has been studied in detail, predominantly by Phillips and co-workers[14] and by us.[15] We have shown that the reaction of *p*-hydroxyphenacyl diethyl phosphate proceeds via a very short-lived triplet state T_1 ($^3\tau$ = 60 ps in wholly aqueous solution) and that the substrate is released concomitantly with the decay of T_1. Questions remain regarding the nature and significance of competing pathways and the effect of substitution of the chromophore on the release of substrates. In particular, the quantum yields for substrate release are often substantially less than unity, suggesting that chemically nonproductive pathways may contribute to the normal photophysical decay of the excited chromophore. Only a very weak fluorescence is observed with this chromophore.[14d]

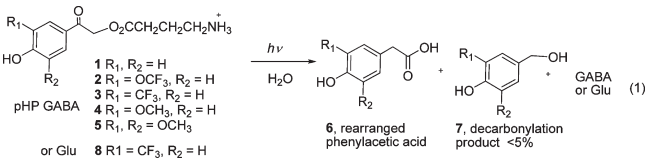

In previous studies, it was demonstrated that the introduction of electron-donating groups such as OCH_3 (**4** and **5**) shifts the π,π^* absorption of the chromophore to longer wavelengths ($\lambda_{max} > 300$ nm), whereas electron-withdrawing meta substituents (CO_2Me or $CONH_2$) have little influence on λ_{max}.[1,9] None of these substituents significantly affected the lifetime of the triplet state in contrast to their effects on the quantum yields.[1,16] Electron-withdrawing groups improve the quantum yields for the photo-Favorskii rearrangement, whereas electron donors are lower vis-à-vis the parent pHP derivatives.

To combine the advantages of the red shift by *m*-methoxy substitution and the improved quantum yields from electron-withdrawing groups, we introduced trifluoromethyl and trifluoromethoxy groups and compared the photochemistry and biological efficacy with those of the methoxy and the unsubstituted pHP GABA analogues. Among the factors that are attendant with introducing a trifluoromethyl substituent are the significant increase in polarity due to the pronounced electron-withdrawing inductive contribution of F,[17] the relatively modest increase in steric size, and the potential improvement in biocompatibility.[18] Although the trifluoromethyl group has rarely been exploited as a substituent on phototriggers,[19] we reasoned that it would modify the reactivity without greatly disturbing the π system of the chromophore. We report here the synthesis and photochemistry of three trifluoromethyl modifications, CF_3O-pHP GABA (**2**), CF_3-pHP GABA (**3**), and CF_3-pHP Glu (**8**), to test this hypothesis. We have also probed the differences between **2** and **3** upon GABA release at the $GABA_A$ receptor using whole-cell patch clamp monitoring of neurons in cortical slices and compared these derivatives with those of our previous study employing unsubstituted pHP GABA (**1**) and *m*-CH_3O-pHP GABA (**4**).[9]

Results and Discussion

Synthetic Studies. The synthetic sequence for **3** shown in Scheme 1 is the general route used for all three of the new derivatives. Benzyl protection of commercially available 4-bromo-2-(trifluoromethyl)phenol (**9**) with $BnBr/K_2CO_3/CH_3CN$, followed by acetylation with a Stille protocol[20] using $Pd(PPh_3)_4$/tributyl(1-ethoxyvinyl)stannane in toluene, and hydrolysis of the resulting enol ether gave the fluorinated

(4) (a) Hess, G. P. Reference 1, pp 205−231. (b) Callaway, E. M.; Yuste, R. *Curr. Opin. Neurobiol.* **2001**, *12*, 587–592. (c) Pettit, D. L.; Augustine, G. J. *Ion Channel Localization* **2001**, 349–370.
(5) (a) Park, C.-H.; Givens, R. S. *J. Am. Chem. Soc.* **1997**, *119*, 2453–2463. (b) Geibel, S.; Barth, A.; Amslinger, S.; Jung, A. H.; Burzik, C.; Clarke, R. J.; Givens, R. S.; Fendler, K. *Biophys. J.* **2000**, *79*, 1346–1357.
(6) (a) Kötting, C.; Kallenbach, A.; Suveyzdis, Y.; Wittinghofer, A.; Gerwert, K. *Proc. Natl. Acad. Sci.* **2008**, *105*, 6260–6265. (b) Warscheid, B.; Brucker, S.; Kallenbach, A.; Meyer, H. M.; Gerwert, K.; Kötting, C. *Vib. Spectrosc.* **2008**, *48*, 28–36. (c) Du, X.; Frei, H.; Kim, S.-H. *J. Biol. Chem.* **2000**, *275*, 8492–8500.
(7) Zou, K.; Cheley, S.; Givens, R. S.; Bayley, H. *J. Am. Chem. Soc.* **2002**, *124*, 8220–8229. Zou, K.; Miller, W. T.; Givens, R. S.; Bayley, H. *Angew. Chem., Int. Ed.* **2001**, *40*, 3049–3051.
(8) Specht, A.; Loudwig, S.; Peng, L.; Goeldner, M. *Tetrahedron Lett.* **2002**, *43*, 8947–8950.
(9) Conrad, P. G. II; Givens, R. S.; Weber, J. F. W.; Kandler, K. *Org. Lett.* **2000**, *2*, 1545–1547.
(10) Givens, R. S.; Jung, A. H.; Park, C.-H.; Weber, J. F. W.; Bartlett, W. *J. Am. Chem. Soc.* **1997**, *119*, 8369–8370.
(11) Givens, R. S.; Weber, J. F. W.; Conrad, P. G.; Orosz, G.; Donahue, S. L.; Thayer, S. A. *J. Am. Chem. Soc.* **2000**, *122*, 2687–2697.
(12) Sul, J.-Y.; Orosz, G.; Givens, R. S.; Haydon, P. G. *Neuroglia Biol.* **2004**, *1*, 3–11.
(13) The blue shift of the chromophore of the product (*p*-hydroxyphenyl)-acetic acid to below 300 nm avoids competitive absorption with pHP and thus permits 100% conversion of pHP derivatives at incident wavelengths >300 nm. The "photo-Favorskii rearrangement" was first reported by Anderson and Reese: Anderson, J. C.; Reese, C. B. *Tetrahedron Lett.* **1962**, 1–4.
(14) (a) Chen, X.; Ma, C.; Kwok, W. M.; Guan, X.; Du, V.; Phillips, D. L. *J. Phys. Chem. A* **2006**, *110*, 12406–12413. (b) Chen, X.; Ma, C.; Kwok, W. M.; Guan, X.; Du, V.; Phillips, D. L. *J. Phys. Chem. B* **2007**, *111*, 11832–11842. (c) Ma, C.; Kwok, W. M.; Chan, W. S.; Du, Y.; Kan, J. T. W.; Toy, P. H.; Phillips, D. L. *J. Am. Chem. Soc.* **2006**, *128*, 2558–2570. (d) Ma, C.; Kwok, W. M.; Chan, W. S.; Zou, P.; Kan, J. T. W.; Toy, P. H.; Phillips, D. L. *J. Am. Chem. Soc.* **2005**, *127*, 1463–1472. (e) Ma, C.; Zou, P.; Kwok, W. M.; Chan, W. S.; Kan, J. T. W.; Toy, P. H.; Phillips, D. L. *J. Org. Chem.* **2004**, *69*, 6641–6657. (f) Ma, C.; Kwok, W. M.; Chan, W. S.; Zou, P.; Phillips, D. L. *J. Phys. Chem. B* **2004**, *108*, 9264–9276.
(15) Givens, R. S.; Heger, D.; Hellrung, B.; Kamdzhilov, Y.; Mac, M.; Conrad, P. G.; Cope, E.; Lee, J. I.; Mata-Segreda, J. F.; Schowen, R. L.; Wirz, J. *J. Am. Chem. Soc.* **2008**, *130*, 3307–3309.
(16) (a) Givens, R. S.; Conrad, P. G., II; Yousef, A. L.; Lee, J.-I. Photoremovable protecting groups. *CRC Handbook of Organic Photochemistry and Photobiology*, 2nd ed.; CRC Press: Boca Raton, FL, 2004; pp 69/1−69/46. (b) Givens, R. S.; Weber, J. F. W.; Jung, A. H.; Park, C.-H. New photoprotecting groups: desyl and p-hydroxyphenacyl phosphate and carboxylate esters. *Methods Enzymol.* 1998, *291* (Caged Compounds), 1−29.
(17) Pauling, L. *The Nature of the Chemical Bond*; Cornell University Press: Ithaca, NY, 1960.
(18) Ojima, I. *ChemBiolChem* **2004**, *5*, 628–635.
(19) Specht, A.; Goeldner, M. *Angew. Chem., Int. Ed.* **2004**, *43*, 2008–2012.
(20) Stille, J. K. *Angew. Chem., Int. Ed. Engl.* **1986**, *25*, 508–524.

SCHEME 1. Synthetic Strategy for Trifluoromethyl-Substituted pHP Amino Acids

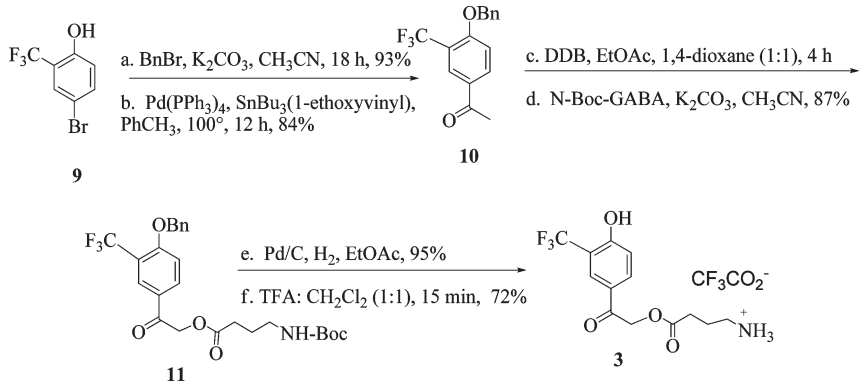

TABLE 1. UV Spectral Data, pK_a, and Disappearance Quantum Yields[a] for pHP GABA Derivatives 1−5 and CF_3−pHP Glu (8)

pHP	λ_{max} (log ε)	pK_a[b]	$\phi_{dis}(H_2O)$[c]	ϕ_{dis}(pH 7.3)[d]	ϕ_{dis}(pH 8.2)[e]	λ_{max} (log ε), pH 9.0	ϕ_{dis}(pH 9.0)[f]
1[g]	282 (4.16), 325 sh	8.0	0.20	0.20	0.09	326 (4.06)	0.0041
2	274 (4.20), 331 (3.54)	6.7	0.09[h]	0.06	0.02	332 (4.18)	0.0058
3	328 (4.11)[i]	5.5	0.17	0.12	0.08	328 (4.14)	0.0081
4	279 (3.97), 307 (3.90), 341 sh	7.85	0.06	NA	0.02	348 (4.05)	NA
5	303 (3.90), 355 (3.55)	7.78	0.03[g]	NA	NA	366 (4.30)	NA
8	328 (4.11)[h]	5.5	0.18	NA	0.11	328 (4.11)	0.0067

[a]Quantum yields for the appearance of GABA were within ±10% of the disappearance quantum yields for pHP GABA, ϕ_{dis}. [b]pK_a's were determined titrimetrically (see the Supporting Information). [c]Deionized water, pH = 7.0. [d]0.01 M HEPES, adjusted to pH = 7.3, [e]0.01 M HEPES adjusted to pH = 8.2. [f]0.01 M Tris adjusted to pH 9.0, 0.1 M $LiClO_4$, irradiation λ = 350 nm. [g]See ref 1a, Chapters 1.3 and 2. [h]An identical value was obtained with oxygen-purged solutions (Ar, 30 min). [i]The pK_a (5.5) is below the pH for this pHP GABA derivative.

acetophenone **10**. The Stille coupling of protected *p*-bromophenols to stannyl vinyl ethers served as a high-yielding, general route for us to synthesize a variety of *p*-hydroxyacetophenones (pHA)[21] as opposed to traditional acylation methodology. α-Bromination with dioxane dibromide in dichloromethane (DDB/CH_2Cl_2), followed by esterification with *N*-Boc-protected GABA and deprotection of the phenol and amine groups with Pd/C (10% w/w)/H_2 in EtOAc and 1:1 TFA/CH_2Cl_2, respectively, afforded **3** in 55% overall yield from **9**. Essentially the same route was followed for the syntheses of **2** (57%) and **8** (38%).

Photochemical Studies. All three derivatives, **2**, **3**, and **8**, quantitatively released the amino acid upon irradiation at λ > 300 nm in aqueous media under ambient conditions. The Favorskii rearrangement products **6** (R_1 = OCF_3 or CF_3; R_2 = H) along with small amounts of the minor product, *p*-hydroxybenzyl alcohols **7**, were characterized by ^{1}H, ^{13}C, and ^{19}F NMR and mass spectral analysis and, for certain cases, by comparison with authentic samples. In the case of the formation of *p*-hydroxy-*m*-(trifluoromethoxy)benzyl alcohol **7** from **2**, for example, the reaction products were also verified by NMR analysis after spiking the photolysis mixture with an independently synthesized sample of **7**. Another potential photohydrolysis byproduct, 2-hydroxy-1-[4-hydroxy-3-(trifluoromethoxy)phenyl]ethanone (**12**), which is structurally related to products that had been reported by others,[22] was shown not to be present by ^{1}H and ^{13}C NMR analysis by the addition of an authentic sample to the photolysis mixture.

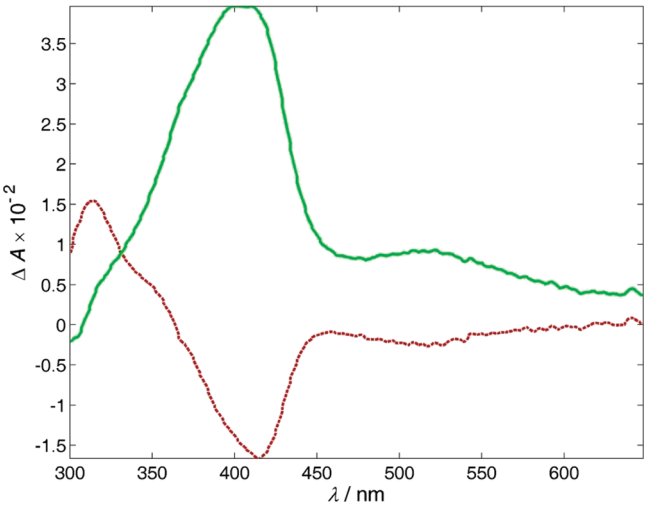

FIGURE 1. Species spectra of the singlet (absorption and stimulated emission; red, dotted) and triplet (absorption; green, solid) of **1** in water determined by global analysis of the spectra taken with delays of 0.6−15 ps using a monoexponential rate law for fitting.

Quantitative analyses of the major products GABA and the substituted (*p*-hydroxyphenyl)acetic acid, along with unreacted caged GABA, were accomplished using LC/MS/MS equipped with a C18 RP column (mobile phase gradient 1:1 MeOH/H_2O with added $NH_4 \cdot HCO_2$ and acetaminophen as the internal standard). This highly sensitive LC/MS/MS method for quantitative analysis coupled with rapid data collection made possible the accurate analyses of the reaction profiles for quantum yields, quenching experiments, and media effects on the photochemistry at low conversions and using less than a few milligrams of caged GABA. The quantum yield data are given in Table 1.

(21) Stensrud, K. F.; Heger, D.; Šebej, P.; Wirz, J.; Givens, R. S. *Photochem. Photobiol. Sci.* **2008**, *7*, 614–624.
(22) Zhang, K.; Corrie, J. E. T.; Munasinghe, R. N.; Wan, P. *J. Am. Chem. Soc.* **1999**, *121*, 5625–5632.

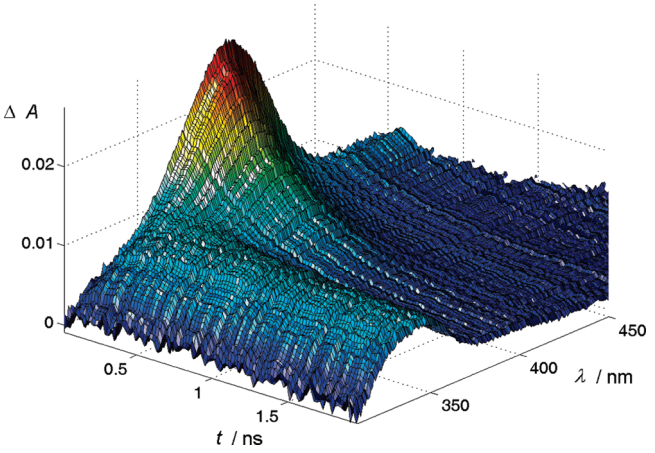

FIGURE 2. Pump−probe spectra of **2** in water, reconstructed after factor analysis in the time range from 20 ps to 1.96 ns using the species spectra shown in Figure 3.

The photorelease quantum yield of the trifluoromethoxy derivative **2** in an unbuffered aqueous solution ($\phi = 0.09$) is approximately twice that of the methoxy (**4**) or dimethoxy (**5**) counterparts, whereas that of the trifluoromethyl analogue **3** ($\phi = 0.17$) is nearly the same as that of the parent pHP GABA **1**. Stern−Volmer studies at high concentrations of sorbate quenched these reactions, confirming a short-lived triplet reactive intermediate for pHP esters **2** and **3** (see the Experimental Section) in accordance with our earlier results with **1**.[5,9,23] In a HEPES buffer, pH 7.3 (1−9 mM pHP GABA), the quantum yields were slightly lower, which we attribute to pH and salt effects,[24] a suggestion supported by dramatic changes in the quantum yields when the pH is varied. In the absence of buffers, the pH of the photolysis solution decreases with increasing conversion because of the production of two carboxylic acids of lower pK_a's than the pHP phenol. Quantum yields are dependent on the pH of the solution (vide infra).

Increasing the pH to 8.2 or 9, values significantly above the pK_a's of **2** or **3**, lowered the quantum yields by half or more. The observed strong red shift in the absorption spectra at the higher pH is due to the formation of conjugate bases of these phenolic chromophores, and photorelease from these is decidedly less efficient, as was reported earlier.[15,16]

None of these photoreactions is appreciably quenched by air, a manifestation of the very short lifetimes and high reactivities of the pHP triplet excited states. The inefficiency of O_2 quenching was tested by purging the photolysis solution with argon (see **2**, Table 1).

Time-Resolved Pump−Probe Studies. Picosecond transient absorption spectra were obtained for compounds **1**−**5**. The samples were excited at 266 nm (pulse width 200 fs) and probed by delayed supercontinuum pulses covering a range of 300−650 nm. The main features in the transient spectra of **1** up to 15 ps are the absorptions by the excited singlet and triplet states of the pHP chromophore, which are shown for **1** in Figure 1. Global analysis of the spectral evolution with increasing delay up to 2 ns of the probe pulse provided the singlet and triplet lifetimes, $^1\tau = 2.3$ ps and $^3\tau = 0.34$ ns, respectively.

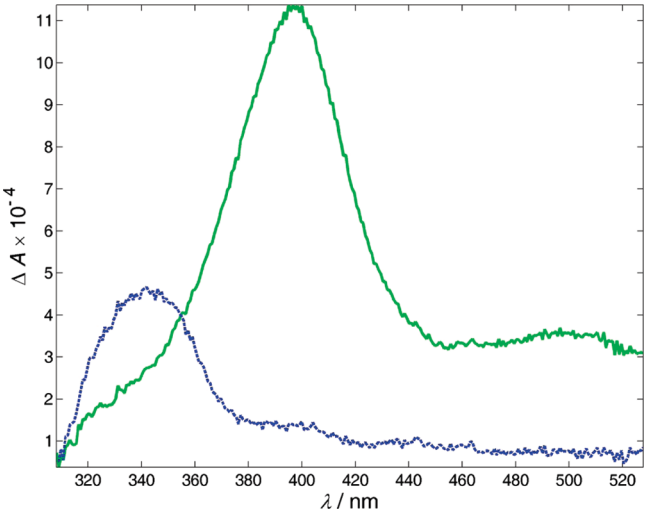

FIGURE 3. Species spectra attributed to the triplet (solid, green) and the conjugate base (anion) of pHP (see text) formed from the triplet (dotted, blue) of **2** in water determined by global analysis of the spectra using a biexponential fit. These spectra are equal to those taken at delays of 4 ps and 1.96 ns, respectively.

TABLE 2. Singlet ($^1\tau$) and Triplet ($^3\tau$) Lifetimes and Rate Constants Obtained from Pump−Probe and Stern−Volmer Measurements

pHP GABA	$^1\tau$/ps	$^3\tau$/ns	ϕ_{dis}[a]	$k_{pF}/10^8$ s^{-1}[b]
		H_2O		
1	2.3	0.34	0.20	6.00
2		0.46	0.09	1.98
3		0.39	0.17	4.42
4		0.77	0.06	0.78
		10% CH_3CN/H_2O[c]		
2		0.71		
3	3.3	0.39		
4	4.6			
5	3.7	0.36		

[a]See Table 1. [b]Calculated as $k_i = \phi_i/^3\tau$, where ϕ_{dis} is the quantum yield for the pHP GABA disappearance and k_{pF} is the rate constant for the photo-Favorskii process (see Scheme 2). [c]Data were obtained by pump−probe spectroscopy. Approximately 10% CH_3CN was added to ensure complete solubility of the substituted pHP GABA.

TABLE 3. Effect of H_2O on the Rate of Disappearance of the 390−400-nm Band

$^3k_{dis}$/s^{-1}	mol % H_2O[a]	refs[b]
1.6×10^{10}	100.00	this work
9.95×10^9	95.14	this work
3.45×10^9	89.77	Phillips[14]
3.30×10^9	74.53	this work
1.89×10^9	66.11	Phillips[14]
1.25×10^9	55.64	Phillips[14]
7.81×10^8	49.38	Phillips[14]
4.17×10^8	34.05	Phillips[14]
1.11×10^8	24.54	Phillips[14]
3.84×10^7	15.03	Hellrung
1.15×10^7	10.00	Hellrung
6.56×10^6	7.51	Hellrung
2.72×10^6	5.04	Hellrung
2.62×10^5	0.00	Hellrung

[a]CH_3CN was the cosolvent. [b]Data are combined from this work and from previous studies (Hellrung, B.; Wirz, J., unpublished, and Phillips and co-workers[14] as indicated).

(23) (a) Conrad, P. G. II; Givens, R. S.; Hellrung, B.; Rajesh, C. S.; Ramseier, M.; Wirz, J. *J. Am. Chem. Soc.* **2000**, *122*, 9346–9347. (b) See also: Chan, W. S.; Ma, C.; Kwok, W. M.; Phillips, D. L. *J. Phys. Chem. A* **2005**, *109*, 3454–3469. (c) Chan, W. S.; Ma, C.; Kwok, W. M.; Phillips, D. L. *J. Org. Chem.* **2005**, *70*, 8661–8675.

(24) We have found a salt effect on several of these photorelease reactions, which we will report on more fully at a later time.

The transient spectrum of the excited singlet state exhibits an absorption maximum around 315 nm, but it is overlaid by stimulated emission, which is responsible for the negative peak observed at 420 nm (dotted red curve in Figure 1). Because both of these transitions arise from the same state, they exhibit the same kinetic behavior. Singlet−triplet intersystem crossing (ISC) results in a rise of the strong triplet−triplet absorption band of ^{3}**1** at 400 nm (Figure 1). A similar 400-nm absorption band was observed under conditions similar to those of pHA, which is quenchable with potassium sorbate and has previously been assigned as being due to the triplet−triplet absorption for pHA.[23] Similar triplet−triplet absorption spectra were observed for the other four

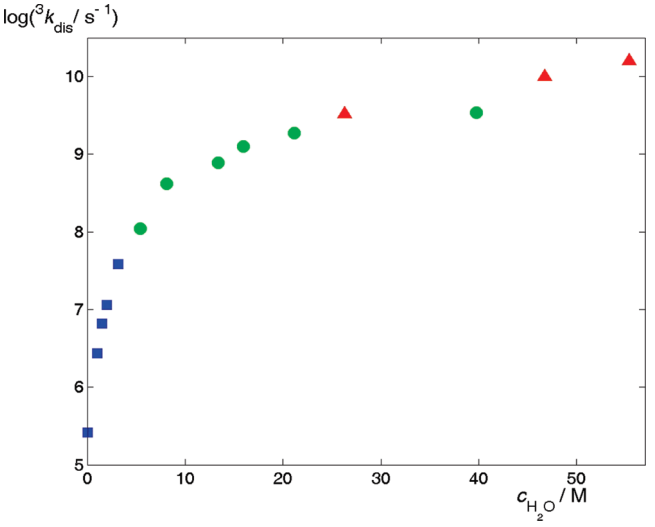

FIGURE 4. Effect of H_2O on the rate of disappearance of the 390−400-nm band (the blue squares are from Hellrung and Wirz, the green circles are from Phillips et al.,[14] and the red triangles are this work).

pHP derivatives, i.e., a maximum at 400−420 nm with a shoulder at ∼520 nm. Sorbate quenching of the 400-nm bands of the pHP derivatives likewise established them as triplet−triplet absorptions in agreement with our previous studies[15,23a] and those by the Phillips group[14,23b,23c] derived from time-resolved transient absorption and resonance Raman spectral analyses with pHP phosphate and carboxylate esters.

The pump−probe time scan from 20 ps to 1.96 ns for **2** in water is shown in Figure 2, and the species spectrum attributed to the triplet of **2** is given in Figure 3 (solid green line). Also shown in Figure 3 is the spectrum of a species that persists after the decay of the triplet, $\lambda_{max} \approx 340$ nm (dotted blue line). A decay rate constant of $k_{dec} \sim 6.5 \times 10^6$ s^{-1} was determined for the 340-nm transient by nanosecond flash photolysis of **2** in water containing ca. 10% acetonitrile, similar to the results obtained with pHP phosphates.[15,23]

In order to identify the 340-nm transient, we examined the transient spectra of pHA in aqueous solution. Pump−probe spectra showed the formation of both the 400-nm absorption band due to the triplet and a 340-nm transient lifetime exceeding that accessible by the delay line (≤2 ns). Nanosecond LFP of pHA showed that neither the lifetime nor the amplitude of the 340-nm transient were affected by the addition of up to 10 mM sorbate, whereas the lifetime of the 400-nm triplet transient was reduced by more than 10-fold ($k_q \approx 2 \times 10^9$ M^{-1} s^{-1}). Thus, the 340-nm transient is not a triplet. It showed first-order decay kinetics ($^1\tau \sim 10^{-5}$ s^1), and with the addition of 10^{-4} M HCl in a solution containing 10 mM sorbate, the lifetime of the 340-nm transient was quenched ($k_{Hsorb} = 4.6 \times 10^9$ M^{-1} s^{-1}), suggesting that it is the ground-state anion of pHA. Indeed, the onset of the absorption by pHA$^-$ follows the shape of the 340-nm transient down to 350 nm, but it continues to rise to its maximum at 325 nm. The shape of the transient absorption (Figure 3, dotted blue line) with an apparent maximum

SCHEME 2. Competing Photo-Favorskii and Deprotonation of pHP Esters

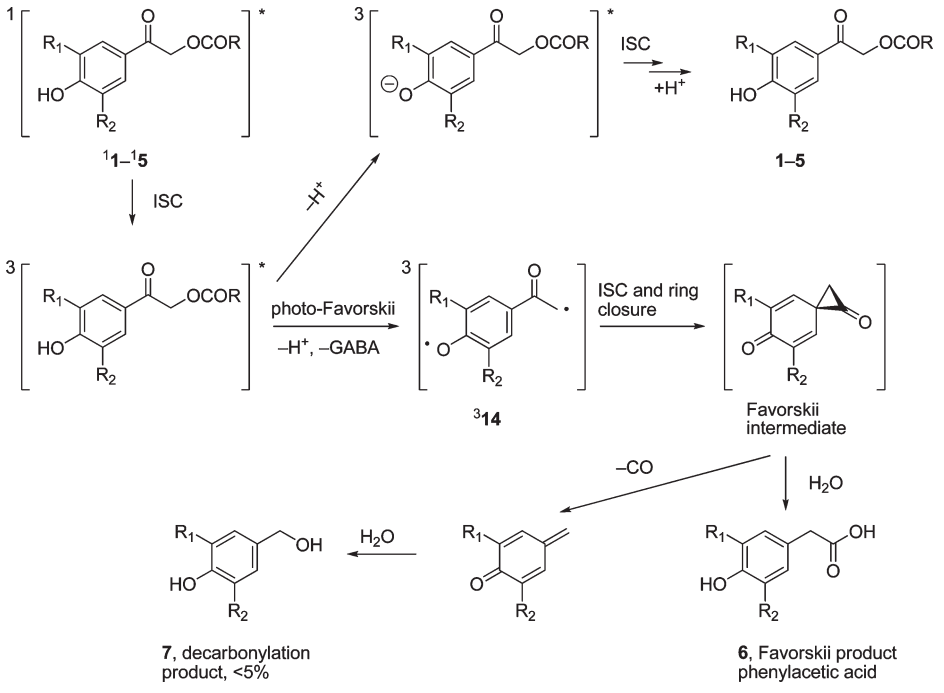

TABLE 4. *C* log *P* and EC_{50} Values for Fluoro-pHP GABA 2 and 3

pHP	ϕ_{dis}(1-octanol)	*C* log *P*	EC_{50} (μM)[a]
1	0.12	1.19	
2	0.14	1.93, −1.59[b]	49.2
3	0.10	2.02, −1.90[a]	119.8
4	0.042[c]	−3.38	93.4

[a]Effective concentration for 50% activity. See Figure 7. [b]This value is for the conjugate base of **2**, which predominates at pH 7.3. [c]The solvent was 1-pentanol.

at 340 nm is, however, distorted by the onset of absorption by ground-state pHA below 350 nm.

On the basis of Förster's cycle,[25] triplet excited pHA is predicted to be a moderately strong acid, $pK_a \approx 3.6$.[23a] Ionization of triplet pHA in aqueous solution occurs on a time scale of 10 ns.[23c] This explains why quenching of the pHA triplet with up to 10 mM sorbate does not reduce the yield of the ground-state anion absorbing at 340 nm. Acceptor-substituted pHP derivatives such as the pHP GABAs are likely to have a somewhat lower pK_a. Thus, we attribute the pathway competing with Favorskii rearrangement to triplet-state deprotonation of the phenol,[15,23,25] forming the triplet conjugate base of pHP GABA. Subsequent ISC of the anion triplet and neutralization regenerate the starting pHP ester. The overall process must be viewed as a competing "energy-wasting" sequence responsible for the diminished release quantum yields. This and other competing pathways from the triplet lower the release yield in the order $R_2CO_2^- < R_2O_2PO_2^- < RSO_3^-$. Together, these results suggest that better leaving groups influence the partitioning of the triplet more favorably toward the photo-Favorskii pathway.[14d,15,23a,26]

Thus, the short triplet lifetimes of less than a nanosecond in wholly aqueous solution observed for the pHP esters can be attributed to a facile heterolysis of the leaving group. As reported earlier, water has a significant effect on the rate and quantum yield.[21] For example, the triplet lifetime of pHP diethyl phosphate with its better leaving group decreases dramatically as the proportion of water in acetonitrile is increased (Table 3 and Figure 4).[14,15,23a] Nevertheless, the quantum yields for the disappearance of the pHP phosphate and the appearance of the rearranged phenylacetic acid remain significantly below unity. These observations confirm that an additional process is competing with the rearrangement/release process in aqueous environments.

For the rearrangement pathway, as we had previously proposed, an adiabatic C−O bond heterolysis is accompanied by deprotonation of the phenol[15,21,23] to generate the oxyallyl−phenoxy triplet biradical ^{3}**14** (λ_{max} = 445 and 420 nm; $\tau \sim 0.6$ ns). This biradical was also observed, but barely detectable, in the pump−probe absorption spectra of the present series (see the Supporting Information for the biradical triplet−triplet transient absorption spectrum for ^{3}**14**). Its weak signals were overlaid by the strong triplet absorptions, which are longer-lived than those for **1** (Table 2). The two competing pathways for pHP GABA are summarized in Scheme 2.[15,21]

Finally, the effects of the pH on the quantum yields prompted further investigations of **2** and **3**. Photolysis of

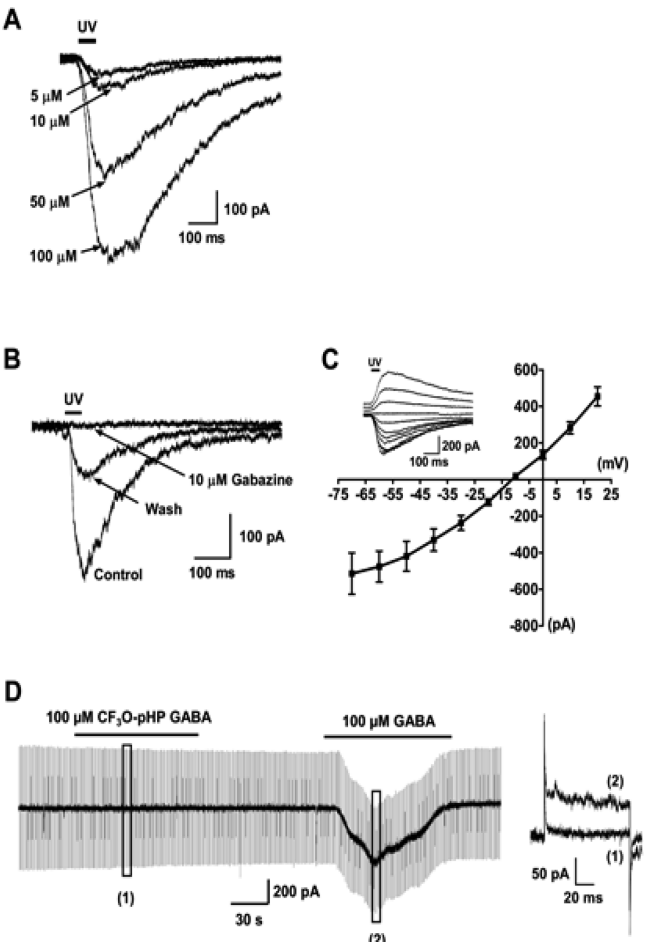

FIGURE 5. Dose-response of **2** photolysis. (A) Sample traces of whole-cell currents elicited by the photolysis of **2** with 50-ms UV light pulses (horizontal bar; UV). (B) Specific $GABA_A$ receptor antagonist Gabazine (10 μM) completely blocked currents evoked by the photolysis of **2** (100 μM, flash duration 10 ms). Washout of Gabazine partly restored the initial response. (C) Current−voltage curve: Peak amplitudes of responses are plotted versus the holding membrane potential (−70 to +20 mV; n = 3 neurons). The inset shows sample traces at the various holding potential (100 μM **2**, flash duration 50 ms). (D) **2** having no effect on the holding currents or membrane input resistance. Perfusion with ACSF containing 100 μM **2** for 2 min (horizontal bar) did not change the membrane input resistance (1), whereas bath application of 100 μM GABA for 2 min decreased the membrane input resistance because of the activation of $GABA_A$-activated chloride channels.

the conjugate base of the trifluoromethyl pHP GABA derivatives demonstrated a decided diminution in the quantum yields at pHs above the pK_a of the phenolic group. The lower photoreactivity of the phenolates may follow a completely different mechanistic pathway, although the photoproducts remain the same.

The replacement of methyl with trifluoromethyl is accompanied by a significant increase in the lipophilicity of the two GABA derivatives for **2** and **3**, nearly doubling *C* log *P*, as determined by partitioning between 1-octanol and water, compared with the unsubstituted pHP GABA (Table 4). The effects of increased lipophilicity on the photoreactions of **2** and **3** were reflected by the quantum yields in 1-octanol and in mixtures of CH_3CN/H_2O or dimethyl sulfoxide (DMSO)/H_2O. In 1-octanol, **2** and **3** had quantum yields for the

(25) Klán, P.; Wirz, J. *Photochemistry of Organic Compounds*; Wiley: Chichester, U.K., 2009.
(26) Cope, E. Ph.D. Thesis, The University of Kansas, Lawrence, KS, 2008, unpublished results .

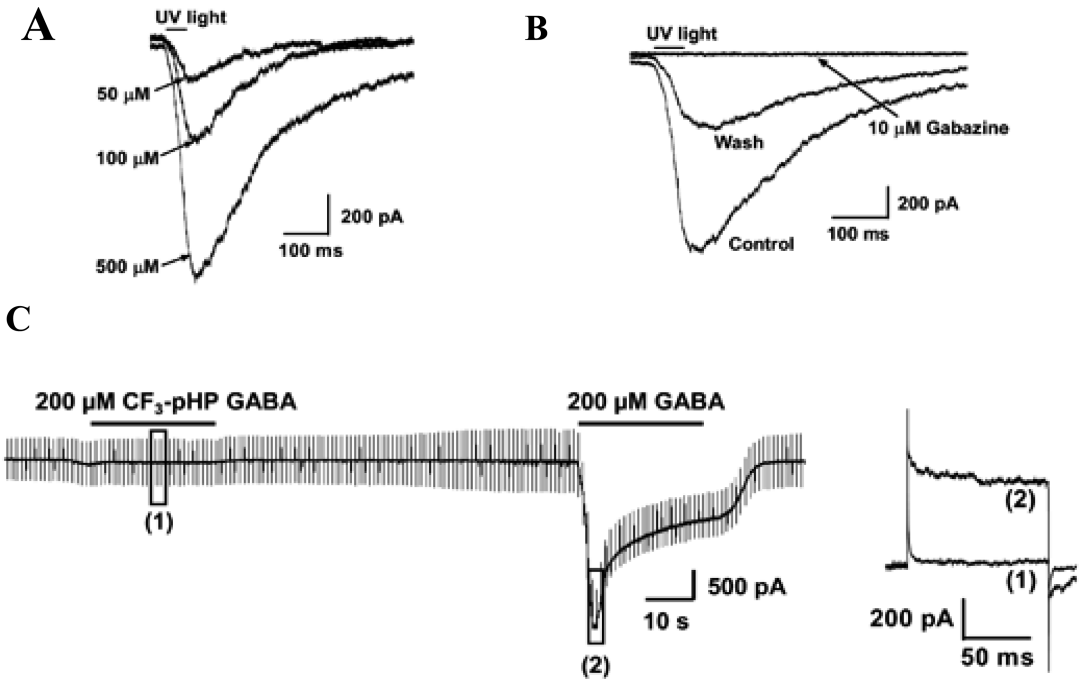

FIGURE 6. Dose−response of **3** photolysis. (A) Examples of membrane current responses of a neuron upon photolysis of **3** at concentrations of 50, 100, and 500 μM. (B) Responses elicited by the photolysis of **3** (200 μM) blocked by the specific $GABA_A$ receptor antagonist Gabazine (10 μM). Upon 15 min washout of Gabazine, the response partially recovered. These results indicate that photochemically released GABA from **3** activated $GABA_A$ receptors. (C) **3** (200 μM, application during the black bar) itself having no effect on the holding currents or the membrane input resistance, indicating that **3** itself did not activate $GABA_A$ receptors. In contrast, in the same neuron, 200 μM GABA elicited a strong inward current and decreased the input resistance, as indicated by an increase in the amplitude of the injected current necessary to produce a 5 mV membrane potential depolarization (example traces to the right).

disappearance of 0.14 and 0.10, respectively. In aqueous−organic mixed solvents, the quantum yields increased with an increase in the water content in accordance with earlier observations with mixed acetonitrile/H_2O solvent mixtures.[14,15,21,23] Typically, for biologically benign solvents like CH_3CN or DMSO, the quantum yield for **2** increased by a factor of 4 upon the addition of 10% (v/v) H_2O, i.e., increasing from 0.03 in dry CH_3CN to 0.12 in 10% H_2O/CH_3CN. Above 25% H_2O, the quantum yields remained relatively constant.

Results of the CF_3 Substituent Effect on the Photorelease of GABA in Biological Studies. The trifluoromethoxy- and trifluoromethyl-caged pHP GABAs **2** and **3** were tested for their efficacy in whole-cell patch clamp studies in neurons in cortical slices of mice[27] and compared with earlier results for the methoxy (**3**) and dimethoxy (**4**) GABA derivatives.[9] Local photolysis with short UV light pulses (10−50 ms) delivered through a small-diameter optical fiber produced transient whole-cell inward currents. As shown in Figures 5 and 6, increasing the concentration of the photolyzed derivative generated currents of larger amplitude and longer duration.

To elucidate whether photolysis of these new derivatives was evoking activation of the $GABA_A$ receptor, the effect of the specific $GABA_A$ receptor antagonist SR 95531 (Gabazine; Tocris, Ellisville, MI) on the photolysis responses and the reversal potential of **2** and **3** was determined. SR 95531 completely abolished photolysis-induced membrane currents (10 μM; Figures 5B and 6B), indicating that the response is mediated by activation of the $GABA_A$ receptor. Current−voltage relationships of responses revealed a reversal potential of −14.2 ± 2.9 mV (n = 3; Figure 5C) for **2**. This value is close to the theoretical value of −20 mV as calculated by the Nernst equation for the chloride concentration between internal (60 mM) and external (133 mM) solutions. Taken together, these results demonstrate that **2** and **3** photolysis-evoked membrane currents are mediated by specifically activating the $GABA_A$ chloride receptor channel.

To determine whether nonphotolyzed **2** could act as an agonist for $GABA_A$ receptors, the effect of **2** on the membrane input resistance was measured by monitoring current responses to short 5 mV depolarizations from a holding

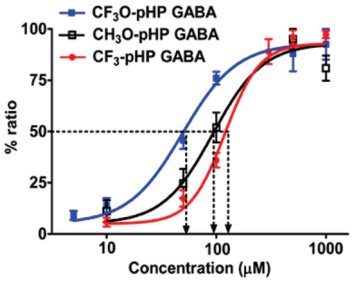

FIGURE 7. Comparison of $GABA_A$ receptor activation by rapid photolysis of pHP GABA. Dose−response curves for **2** (blue, n = 7 neurons), **3** (red, n = 6 neurons), and **4** (black, n = 6 neurons) with **4** population data of the peak currents normalized to the maximum peak response. Data were fitted by Hill's equation to yield EC_{50}. EC_{50} and Hill's coefficient values were as follows: **2**, 49.2 μM, 1.8, n = 7 neurons; **4**, 93.4 μM, 1.9, n = 6; **3**, 119.8 μM, 2.73, n = 6.

(27) Kim, G.; Kandler, K. *Nat. Neurosci.* **2003**, *6*, 282–290.

potential of −70 mV in the presence and absence of GABA (100 μM) or **2** (100 μM). As expected, GABA (100 μM) reduced the membrane input resistance because of its activation of $GABA_A$ chloride channels. In contrast, **2** had no effect on the membrane input resistance (Figure 5 D), indicating that only photolyzed **2**, but not **2** itself, activates $GABA_A$ chloride receptor channels. A parallel study on **3** gave the same result (Figure 6C).

In order to compare the relative sensitivity of photolyzed **2** and **3** with the other caged GABAs, peak amplitudes of the membrane currents elicited by the photolysis of **2** and **3** at increasing concentrations were plotted as concentration−response curves, which were fitted by Hill's equation. The best-fit curves showed EC_{50} values of 49.2, 119.8, and 93.4 μM for **2**−**4**, respectively (Figure 7 and Table 4), demonstrating that photorelease from **2** is more effective in eliciting GABA responses than either **3** or **4**.

Conclusions

We have shown that the competing "energy-wasting" triplet pathway is the deprotonation of the phenol group in the photolysis of pHP GABA derivatives. In aqueous phase photolyses at low to moderate pH, it is the triplet state that undergoes the photo-Favorskii rearrangement, concomitantly releasing the substrate. The efficiency of the triplet excited-state rearrangement pathway depends on several factors, the most important of which is the nucleofugality of the caged substrate and the pK_a of the chromophore. The carboxylate leaving group, e.g., GABA release, is less effective than phosphates,[5,14−16,21−23] for example, as expressed by the higher quantum yields for phosphate release. In fact, carboxylates are among the least efficient substrates (ϕ_d = 0.04−0.20) that we have reported. Additional factors also influence the partitioning of the pathways, including the water content of the solvent, pH, pK_a of the pHP, and media effects.

Evidence that the conjugate bases are much less efficient chromophores for photorelease was reinforced with both trifluoromethyl derivatives through studies at pH 9.0, well above the pK_a's of the pHP derivatives, and at 350 nm, where only the conjugate base absorbs. Thus, substituents on the chromophore can attenuate the effective pH range and wavelength region available for photorelease by their influence on the pK_a of the *p*-hydroxy group. In the present case, electron-withdrawing substituents on the chromophore sufficiently lower the pK_a to a point where the conjugate base is the only species present at pH 9. Consequently, the quantum yields are depressed to <0.02 because of the poor reactivity of the conjugate base. In a similar manner, photoinduced deprotonation to the conjugate base is an unproductive pathway.

The fluoro substitution did improve the lipophilicity of the chromophore, a feature that may have future implications regarding the transport of caged compounds across membranes in biological studies. A test on the photochemical efficacy in more lipophilic environments such as octanol, acetonitrile, and DMSO showed that photorelease occurs, but the quantum yields improved with added H_2O as a cosolvent, as was the case for acetonitrile/H_2O mixtures.[14c] As a further test, the efficacy of fluorinated pHP GABA derivatives were tested for controlled release of GABA as an agonist at the $GABA_A$ receptor in whole-cell, patch clamp studies with neurons in cortical slices. Photoreleasing GABA from **2** was >50% more effective as an agonist than from its nonfluoro analogue. This was not true for the CF_3 derivative, which was less effective by ca. 30% relative to the *m*-CH_3O−pHP GABA in spite of its greater quantum yield.

Further studies on the complex effects that substitutents have on the photochemical and photophysical properties of the pHP chromophore, including ionic strength and leaving group effects on the partitioning of the two dominant triplet pathways, are needed to more fully understand the efficacy of the pHP phototrigger reaction and are currently being pursued by our groups.

Experimental Section

Quantitative photolysis conditions for the determination of quantum yields and Stern−Volmer quenching constants (K_{SV}) were as follows: The lamp light output (in millieinsteins per minute) was established using the potassium ferrioxalate method.[28] Milligram quantities of caged compounds and caffeine or acetamidophenol were weighed out on a Fisher brand microbalance and dissolved in 4 mL of 18 MΩ ultrapure water; salt solutions of various concentrations, buffers with or without adjusted ionic strengths, or purified organic solvents were then added to a 10 mm × 75 mm quartz tube and vortexed, resulting in a homogeneous solution of the caged compound and internal standard. The same tubes and mixing procedures were employed for actinometry (vide infra). Concentrations of the caged compounds ranged from 1 to 9 mM. At these concentrations, the absorbance was greater than 4 through the excitation range of the 300-nm lamps, assuring the complete absorption by the sample at low conversion over the irradiation wavelength range employed. These tubes were then placed in a Rayonet MGR 100 carousel within a Rayonet photochemical reactor equipped with two 3000-Å, 15-W lamps. Samples of 100 μL were removed at 30-s intervals up to 5 min using a 250-μL microsyringe after vortexing of the reaction tube and the samples diluted to 1 mL with water using 1-mL volumetric flasks. The samples were thoroughly mixed before LC/MS/MS analysis. Each run gave linear time-dependent conversions up to < 20% conversion of the pHP ester.

The same procedures were used for actinometry using the same volumes in the sample tubes. Complete light absorption by the ferrioxalate solutions was accomplished by following the procedure of Hatchard and Parker.[28] A linear response for the light output was also obtained in each series.

Quantitative analysis was achieved by LC/UV or HPLC/MS/MS. The LC/MS/MS instrument was equipped with a triple-quadrupole, electrospray ionization mass spectrometer, outfitted with an autosampler. UV−vis detection consisted of a dual-wavelength detector set at 220 and 240 nm. The reservoirs used were as follows: (A) 99% water, 1% methanol, 10 mM ammonium formate, and 0.06% formic acid; (B) 99% methanol, 1% water, 10 mM ammonium formate, and 0.06% formic acid. The column was of reversed-phase (C18), 4 μm mesh, and 50 mm. Injections of 100 μL were made with an automated sampler for each run for a total of three injections per vial. A mobile phase gradient was utilized to optimize compound separation. The flow rate was set at 300 μL/min. Data analysis was performed using *MassLynx* software. Smoothing functions were used for peak analysis of the chromatographic peaks. Calibration curves to obtain *R* values from linear least-squares

(28) Hatchard, C. G.; Parker, C. A. *Proc. R. Soc. London, Ser. A* **1956**, *235*, 518–536.

regression were determined at concentrations of the reactants and products in photolyses by systematic increases of pHP-caged GABA, free GABA, and *p*-hydroxyphenylacetic acid concentrations to determine correlations with internal standards caffeine or 4-acetamidophenol. The quantum efficiencies were then calculated from the ratio of the reactant or product concentrations to the photons absorbed using the actinometer values obtained as indicated above. A minimum of three independent, quantitative iterations were conducted for each compound to underpin the veracity of reported quantum efficiencies.

The Stern−Volmer quenching method[29] was employed to determine the triplet lifetimes of pHP derivatives. Potassium sorbate served as the quenching agent. Solutions of pHP GABA (0.001−0.01 M) were diluted with sorbate solutions of increasing concentration (0−0.1 M) and photolyzed under the aforementioned conditions to ascertain the changes in quantum efficiencies of GABA release. Stern−Volmer constants, K_{SV}, were determined from the slope of ϕ_0/ϕ vs [Q]. To determine the triplet lifetime, τ^3, the rate of quenching, k_q, was assumed to be the rate of bimolecular diffusion, $k_{diff} = 7.2 \times 10^9\ s^{-1}$ (water). The K_{SV} values in H_2O were 20 M^{-1} for **2** and 33 M^{-1} for **3**.

Femtosecond transient absorption spectra were measured with the pump−supercontinuum probe technique.[30] The sample was excited with a frequency-quadrupled pulse from a Ti/Sa laser system [775 nm, pulse energy 0.8 mJ, full width at half-maximum (fwhm) 150 fs, operating frequency 426 Hz] described previously.[31] The output at 540 nm was frequency-doubled to 266 nm and after compression provided pump pulses with an energy of 1 μJ and a <100 fs pulse width. A probe beam continuum was produced by focusing the 775 nm, 1 mm pulse in front of a CaF_2 of 2 mm path length. The second harmonic (400 nm) of the fundamental generated a supercontinuum probe in the range 270−690 nm. The pump and probe were focused in a 0.2-mm spot on the sample flowing in an optical cell of 0.4-mm thickness. The probe signal was spectrally dispersed and registered with a photodiode array (512 pixels). The pump−probe cross-correlation was well below 100 fs over the whole spectrum. The experimental transient spectra $\Delta A(\lambda,t)$ were corrected for the chirp of the supercontinuum and for the solvent contribution.

Biological Activity. Experimental Determinations. Experimental procedures were in accordance with the U.S. National Institutes of Health guidelines and were approved by the Institutional Animal Care and Use Committee at the University of Pittsburgh. Mice (aged postnatal days 10−11) were anesthetized with isoflurane and decapitated. The brain was quickly removed from the mouse skull and immersed into an ice-cold artificial cerebrospinal fluid (ACSF), which contained 1 mM kynurenic acid and was composed of the following (in mM): 124 NaCl, 26 $NaHCO_3$, 10 glucose, 5 KCl, 1.25 KH_2PO_4, 1.3 $MgSO_4$, and 2 $CaCl_2$ (pH 7.4 when aerated with 95% O_2/5% CO_2). The brain was blocked, and coronal slices (300 μm thick) were obtained from the cortex using a vibrating microtome. Slices were incubated in an interface-type chamber in a 95% O_2/5% CO_2 atmosphere for 1 h at room temperature (20−25 °C) before commencing electrophysiological recordings.

For electrophysiological recordings, slices were transferred to a chamber mounted to a fixed-stage microscope where they were superfused with ACSF solutions at a rate of 2−3 mL/min using a gravity-driven perfusion system. Whole-cell patch clamp recordings were made in voltage-clamp mode using an Axoclamp-1D amplifier with a Digidata-1440A A/D converter under the control of pClamp10. The recording pipettes (resistance of 2−3 MΩ) were constructed from borosilicate glass capillaries using a P-97 puller. Recording pipettes were filled with a pipet solution containing (in mM): 54 D-gluconic acid, 54 CsOH, 56 CsCl, 1 $MgCl_2$, 1 $CaCl_2$, 10 Hepes, 11 EGTA, 0.3 Na-GTP, 2 Mg-ATP, and 5 QX-314 (pH 7.2, 280 mOsm/L). Recordings were taken at a holding potential of −70 mV, unless otherwise specified. Caged compounds and pharmaceutical drugs were dissolved in ACSF immediately before application.

The area around the recorded neuron was illuminated with UV light using an optical-fiber-based system consisting of a fused-silica fiber (inner diameter 20 μm) coupled to a 100-W mercury arc lamp. The duration of the light pulses was regulated by an electronic shutter located between the lamp and the optical fiber. The location of the light spot on the slice was monitored with a CCD camera. Data are presented as mean ± SEM. The results are shown in Figures 4−6.

Acknowledgment. This work was supported by NIH Grant GM069663 (to R.S.G.), Grant R01 GM72910 (to R. S.G.), Grant DC-04199 (to K.K.), the Czech Ministry of Education, Youth and Sport MSM0021622413 and Grant ME090217 (to DH), and the Swiss National Science Foundation (J.W.). We thank Dr. Hellrung for experimental assistance on the effects of H_2O on the pHP GABA rate constants. We thank the reviewers for very constructive critical comments and valuable suggestions on the original manuscript.

Supporting Information Available: Synthetic procedures, ^1H, ^{13}C, and ^{19}F NMR spectra, and HRMS data for **2**, **3**, and **6**−**12**. This material is available free of charge via the Internet at http://pubs.acs.org.

(29) Desilets, D. J.; Kissinger, P. T.; Lytle, F. E. *Anal. Chem.* **1987**, *59*, 1244–1246.
(30) Details for the pump−probe experiments can be found in ref 21.
(31) Müller, M. A.; Gaplovsky, M.; Wirz, J.; Woggon, W.-D. *Helv. Chim. Acta* **2006**, *89*, 2987–3001.